

# Effects of heat treatment on the properties of arc melted AlCuFeNiSi<sub>0.4</sub> and AlCuFeNiTi<sub>0.2</sub> high entropy alloys for engineering applications

Abidemi Adeyoye<sup>1\*</sup>, Patricia Popoola<sup>2</sup>, Ntombi Mathe<sup>3,4</sup>, Olawale Popoola<sup>5</sup>, Modupeola Dada<sup>6</sup>, and Nhlanhla Dhliwayo<sup>7</sup>

<sup>1\*</sup> Tshwane University of Technology, Department of Chemical, Metallurgical and Materials Engineering, 0001, South Africa

<sup>2</sup> Tshwane University of Technology, Department of Chemical, Metallurgical and Materials Engineering, 0001, South Africa

<sup>3</sup> Tshwane University of Technology, Department of Chemical, Metallurgical and Materials Engineering, 0001, South Africa

<sup>4</sup> National Laser Centre, Council for Scientific and Industrial Research, Meiring Naudé Road, Brummeria, Pretoria 0185, South Africa

<sup>5</sup> Center for Energy and Electric power, Electrical Engineering, Faculty of Engineering and Built Environment, Tshwane University of Technology, Pretoria, South Africa

<sup>6</sup> Tshwane University of Technology, Department of Chemical, Metallurgical and Materials Engineering, 0001, South Africa

<sup>7</sup> Tshwane University of Technology, Department of Chemical, Metallurgical and Materials Engineering, 0001, South Africa

**Abstract.** In this study, AlCuFeNiSi<sub>0.4</sub> and AlCuFeNiTi<sub>0.2</sub> high entropy alloys (HEAs) were synthesized using arc melting. The as-cast alloys were heat treated at 750 °C for 4hrs then quenched in water and oil and aged for 6hrs to examine the influence of the quenching media (water and oil) on the microstructural, nanomechanical, corrosion and wear characteristics of the alloys. The XRD results revealed that both alloys had BCC phase and FCC phase structures, where Ti and Al were the BCC stabilizers and Cu and Ni acted as FCC stabilizers. The excellent combination of hardness and elastic modulus of both alloys quenched in water shows that ageing can improve the properties of the alloys. The alloys quenched in water after ageing offered improved properties compared to those quenched in oil for both alloys. The wear resistance was higher in AlCuFeNiSi<sub>0.4</sub> than in AlCuFeNiTi<sub>0.2</sub> attributed to the strengthening mechanism of the alloy. Electrochemical tests also showed that the AlCuFeNiSi<sub>0.4</sub> alloy composition was more corrosion resistant and easier to passivate in 3.5% NaCl. The combined action of the elements in the HEA composition produced surface oxide layers that were more stable and resistant to corrosion. Hence, the heated treated Si<sub>0.4</sub> HEA derivative has the potential to be used as materials in wider corrosive environments in the energy industry.

## 1 Introduction

HEAs (High entropy alloys) are alloys with a minimum of five metallic elements in the range of 5 to 35 atom percent, according to Tung et al. [1]. They have a higher mixing entropy of 1.5R and above, resulting in advantageous single solid solution crystal structures of BCC (body-centered cubic), FCC (face-centered cubic) or HCP (hexagonal close-packed) and other disadvantageous intermetallic crystalline phases [2]. However, most of the reported systems of these alloys tend to form high symmetry single-phase structures like bcc (body-centered cubic), fcc (face-centered cubic) and hcp (hexagonal close-packed) because of their high mixing entropy [3]. These distinctive qualities give the high-entropy alloy its desirable properties for a variety of applications over conventional alloys. HEAs are commonly made

using arc melting, Arc melting is a technique that ensures the homogeneity of all constituent elements in HEAs by producing high temperatures using an electric arc. By avoiding airborne gases and contaminants, contamination is reduced to a minimum. It enables quick solidification, resulting in uniformly fine microstructures. Arc melting is also scalable for large sample button sizes e.g., diameter of about 50 mm and a thickness of 10 mm and also adaptable in shapes e.g., rectangular and button shape [4]. Furthermore, the ideal microstructure of high-performance HEAs is typically obtained by applying extra thermal or mechanical treatment such as friction stir-processing and heavily cold rolling followed by annealing [5]. Most of the extensively investigated arc melted high entropy alloys, with outcomes like high strengths [6], outstanding high temperature softening resistance [7], superior resistance to wear [8], and corrosion [9], were because of either the retained single phase solid solution phases or strengthening second phase after heat treatment. Research has been conducted on the influence of heat treatments such as annealing, quenching, and age hardening on the microstructure and mechanical performances of HEAs [10]. Fazakas, Zadorozhnyy and Louzguine-Luzgin [11] investigated the effect of annealing on the property and structural evolution of  $(\text{AlTi})_{60-x}\text{Ni}_{20}\text{Cu}_{20}\text{Fe}_x$  and  $\text{Al}_{25}\text{Ti}_{25}\text{Ni}_{25}\text{Cu}_{25}$  (substituting  $x$  as 15 and 20) HEAs using induction melting techniques. The as-cast alloys were thermally treated at 1173, 973, and 773 K for 30 mins. The phenomenon of ageing played a vital role in the enhancement of plasticity, hardness, and elastic properties. In another study, Guo et al. [12] investigated the influence of homogenisation treatments on the wear behaviour, corrosion resistance and microstructure of  $\text{AlCoCrFeNiSi}$  HEA. From the results, the author found that the homogenisation treatment done at 1150 °C for 7200 seconds gave the improved properties. Although, Heat treatment significantly influenced the final microstructures and mechanical properties of the alloy. However, the studies carried out do not give a complete picture of phase stability through quenching in these alloys. Unfortunately, there have been limited literature reports on the influence of heat treatment in varied quenching medium on the microstructural evolution and performances of  $\text{AlCuFeNiSi}$  and  $\text{AlCuFeNiTi}$  HEAs compositions fabricated via arc melting. Hence, this research aims to investigate the effects of age treatments on the nanomechanical, wear, corrosion and microstructure behaviour of  $\text{AlCuFeNiSi}_{0.4}$  and  $\text{AlCuFeNiTi}_{0.2}$  HEAs produced via arc melting for engineering structural applications.

## 2 Materials and methods

Bulk HEAs powders with the compositions of  $\text{AlCuFeNiSi}_x$  ( $x = 0.4$ ) represented as sample E4 and  $\text{AlCuFeNiTi}_x$  ( $x = 0.2$ ) represented as sample L2, were first homogenized using a tubular mixer for a duration of 8 h to ensure even elemental distribution [13]. The alloys were synthesized in an inert argon atmosphere of 0.01 atm and remelted multiple times to promote chemical homogeneity [14]. The ingots were approximately 30 x 20 x 6 mm<sup>3</sup>. The as-cast samples were cut into desired shapes and sizes, homogenized at 1023 K for 4 hrs and then allowed to cool naturally to room temperature. Table 1 provides an overview of the heat treatment processes.

Microstructural identifications were analyzed utilizing an optical microscope (OPM), energy dispersive spectroscopy (EDS) and an X-ray diffractometer (XRD). Nanoindentation equipment (Anton-Paar TTX-NHT3) with a constant load profile of 200 mN was utilized to perform Nanomechanical tests. The wear behaviour of the as-aged samples was determined using an Anton Paar TRB3 pin-on-disc Tribometer under ambient temperatures. The wear rates and friction coefficients were examined under nominal or nonabrasive conditions, with an applied load of 10N and 20N and a sliding speed of 200 rpm for 6000 cycles. The Potentiodynamic polarization test was conducted utilizing computer controlled PGSTAT302 (Autolab Potentiostat/galvanostat). A three-electrode configuration cell system was used for

the experiments; the working electrode was the HEAs sample with an exposed area of 1 cm, the reference electrode was AgCl/Ag, and the counter electrode was a platinum rod. Before performing the polarization experiments, the open-circuit potential after an hour was measured, allowing for a steady potential value with a polarization scan rate of 1 mV/s. The measurements were done at room temperature using a 3.5 weight percent NaCl solution as the electrolyte.

**Table 1.** Details of heat treatment process.

Treatments	Methods
As-cast	Arc melting and casting
As-homogenized	Arc melting and casting → homogenized at 750 °C for 4hrs
As-quenched	Arc melting and casting → homogenized at 750 °C for → 4hrs quenched in water and oil
As-Aged	Arc melting and casting → homogenized at 750 °C for → 4hrs quenched in water and oil → aged for 6hrs

## 3 Results and discussion

### 3.1 Microstructure

Figures 1 (a) and (b) show the micrographs of the as-cast AlCuFeNiTi<sub>0.2</sub> and AlCuFeNiSi<sub>0.4</sub> HEAs, respectively. Three distinct regions were identified in both alloys: typical needle-like dendrites (D) with 10 μm and 2 μm in length and width, respectively, bright regions identified as (Cu-rich phases) and grey regions representing interdendrites (ID). EDS results show that the grey regions (ID) are mostly dominated by Al and Ni, while the dendritic regions are enriched with Fe and Si. Figures 2(a) and (b) depict the phase analysis of the AlCuFeNiTi<sub>0.2</sub> and AlCuFeNiSi<sub>0.4</sub>, respectively, after quenching in water and age hardened. According to the analysis, the as-cast samples are composed of a solid solution phase; FCC (face centered cubic) and BCC (body centered cubic) crystal structures. This is due to their elemental composition. Ti and Al were BCC stabilizers while Cu and Ni acted as FCC stabilizers [15] [16] [17]. The as-cast multi-component HEAs are stable if their mixing enthalpy ( $\Delta H_{mix}$ ), difference in atomic radii ( $\delta$ ), and high mixing entropy ( $\Delta S_{mix}$ ) are all present. These parameters range from 5 to 7 kJ.mol<sup>-1</sup>, 22-22.7 pm, and 66.44 J/mol\*k, respectively, for the as-cast AlCuFeNiTi<sub>0.2</sub> HEA and -7 to -8 kJ/mol, and 4 to 4.9 and 83.16 J/mol\*k for the AlCuFeNiSi<sub>0.4</sub> HEA, respectively. While the valence electron concentrations of both as-cast AlCuFeNiTi<sub>0.2</sub> and AlCuFeNiSi<sub>0.4</sub> HEAs are 20.8 and 21.6, confirming the solid solution phases. When the elemental compositions form a single-phase crystalline structure, as determined by VEC values, solid solution formation takes place. More subtle distinctions encourage formation since stable solid solutions were achieved by balancing parameters with the high mixing entropy.

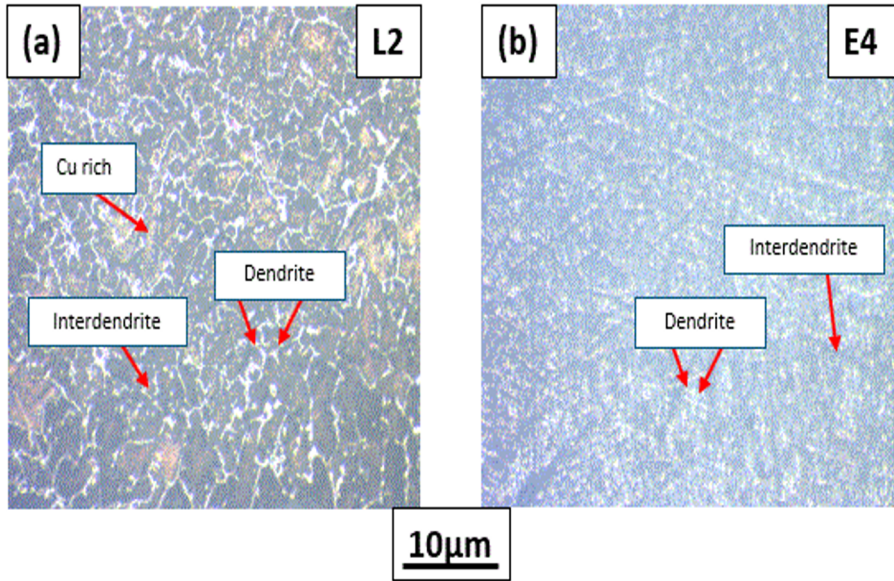


**Fig. 1.** Micrographs of (a) AlCuFeNiTi<sub>0.2</sub> high entropy alloy (b) AlCuFeNiSi<sub>0.4</sub> high entropy alloy.

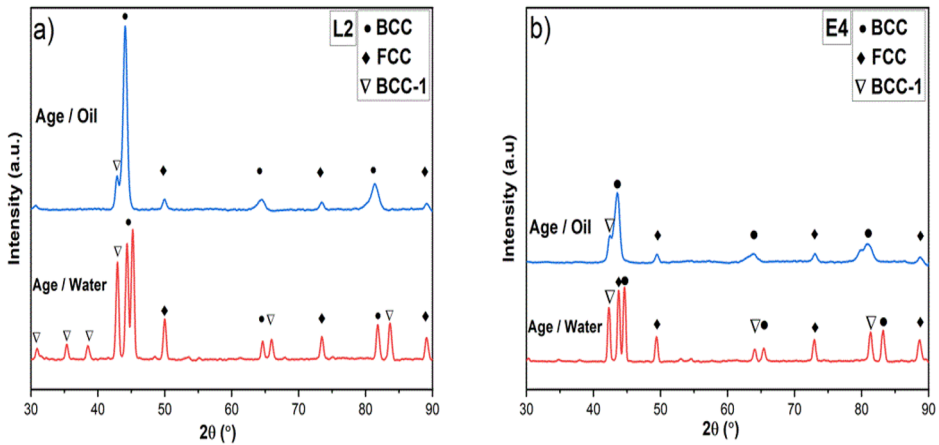


**Fig. 2.** XRD micrograph (a) AlCuFeNiTi<sub>0.2</sub> high entropy alloy (b) AlCuFeNiSi<sub>0.4</sub> high entropy alloy.

### 3.2 Nanomechanical analysis

At an applied load, the responses of the as-cast heat treated HEAs to nanoindentation are shown in Fig. 3. The load-depth curves of the AlCuFeNiSi<sub>0.4</sub> HEA and AlCuFeNiTi<sub>0.2</sub> HEA at 750 °C for 4 hrs holding time, quenched in oil and water, and aged for 6 hrs show that under the applied load of 200 mN, the indentation depth of the as-cast AlCuFeNiTi<sub>0.2</sub> HEA (L2) was greater than the AlCuFeNiSi<sub>0.4</sub> HEA (E4), suggesting a higher deformation resistance of the Si<sub>0.2</sub> HEA (E4) derivative. In the crystal lattice, silicon (Si) causes distortions that impede dislocation movement more than Ti in a HEA composition since Si has larger atoms than Ti. This creates more robust interatomic connections with neighboring atoms,

which makes deformation more challenging in the  $\text{Si}_{0.4}$  derivative HEA. Furthermore, silicon's reduced solubility in the HEA matrix, which causes it to precipitate as tiny particles, strengthening the material and halting dislocation movement. The strengthening mechanism in the  $\text{AlCuFeNiSi}_{0.4}$  HEA could be a result of the formation of the stronger Al–Ti-rich BCC phase in the alloys, which is more resistant to plastic deformation [18]. In addition, these results demonstrate that the alloys quenched in water after ageing for 6 hrs have better properties than those quenched in oil. Interestingly, both alloys showed improved properties in one quenching medium and reduced properties in the other even after ageing for 6 hrs. The reduced hardness and elastic modulus chart of the  $\text{AlCuFeNiSi}_{0.4}$  HEA and  $\text{AlCuFeNiTi}_{0.2}$  HEA heat treated at  $750\text{ }^\circ\text{C}$  for 4 hrs holding time, quenched in oil and water, and aged for 6hrs are shown in Fig. 4.

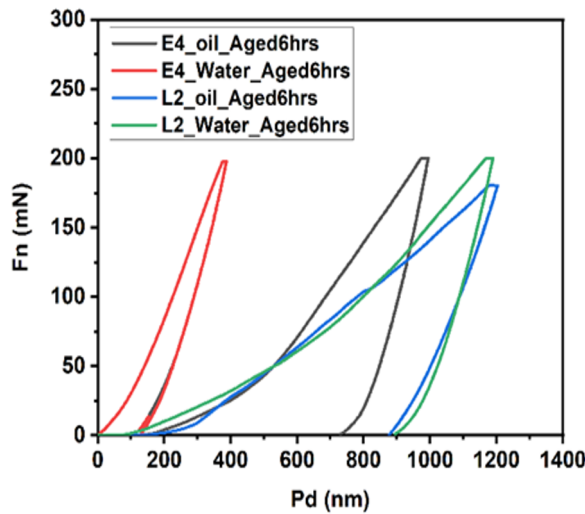


**Fig. 3.** Nanoindentation load-displacement curves of  $\text{AlCuFeNiSi}_{0.4}$  HEA and  $\text{AlCuFeNiTi}_{0.2}$  HEA at  $750\text{ }^\circ\text{C}$  for 4 hrs holding time quenched in oil and water and aged for 6 hrs.

It was observed that the average values of the hardness ( $H$ ) and the reduced elastic modulus ( $E_r$ ) of the as-cast heat treated HEAs showed similar trends. Comparatively, it was observed that the  $\text{Si}_{0.2}$  HEA derivative (E4 sample) quenched in water emerged with the highest hardness and reduced modulus values at 110 GPa and 2000 GPa, respectively, which may have also been responsible for the deformation mechanism of the alloy, which was mostly elastic. The hardness values of L2 were around the same, ranging from 10 GPa to 11 GPa. This indicates that there are different strengthening mechanisms: lattice distortion and solute atoms having several shear moduli than their corresponding solvent atoms, with the solid solution strengthening mechanism playing the most significant role.

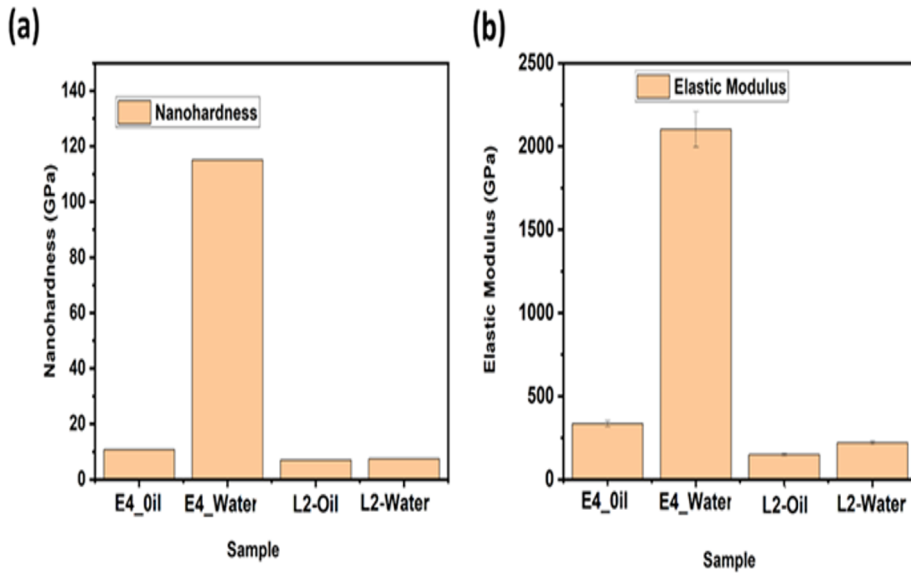


**Fig. 4.** Comparative graph of the average (a) nanohardness and (b) reduced elastic moduli of AlCuFeNiSi<sub>0.4</sub> and AlCuFeNiTi<sub>0.2</sub> HEAs at 750 °C for 4 hrs after quenching treatment in oil and water and aged for 6hrs.

### 3.3 Corrosion analysis

The potentiodynamic polarization curves of the as-cast high entropy alloys in 3.5% NaCl are presented in Fig. 5. It was observed that there is limited passivation for the AlCuFeNiSi<sub>0.4</sub> (E4) and AlCuFeNiTi<sub>0.2</sub> (L2) alloys quenched in oil and aged for 6 hrs because these samples were narrower than those alloys quenched in water and aged for 6 hrs. The corrosion potential of the alloys varies from -1.0324 to -0.2895 V for both alloys. The Si<sub>0.4</sub> HEA derivative had a higher corrosion potential than the Ti<sub>0.2</sub> HEA derivative. This noble corrosion resistance displayed by the AlCuFeNiSi<sub>0.4</sub> (E4) alloy may be attributed to the dominant BCC phase present in its structure and its hardness [19]. The corrosion rates of the HEAs are displayed in Fig. 5b. Generally, the results show a similar trend, the alloys quenched in water and aged for 6 hrs showed the lowest corrosion rates with the smallest wear rates among other alloy compositions. While the Si<sub>0.4</sub> HEA derivative quenched in water and aged for 6 hrs also had the highest corrosion resistance, suggesting that the water quenching medium is necessary for improved hardness, which invariably enhanced the alloys' resistance to corrosion.

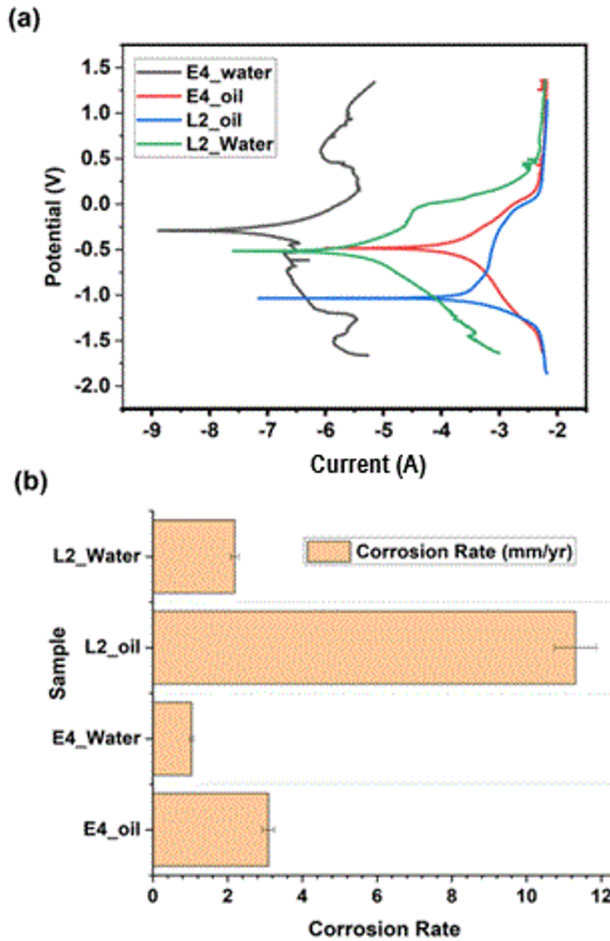


**Fig. 5.** a) Potentiodynamic polarization curves (b) corrosion rate chart of AlCuFeNiSi<sub>0.4</sub> and AlCuFeNiTi<sub>0.2</sub> HEA at 750 °C for 4 hrs after quenching in oil and water and aged for 6 hrs.

### 3.4 Tribological analysis

Tribological experiments were conducted using a ball-on-disc sliding arrangement at room temperature in dry conditions. A steel counter ball with a hardness value of 1550 Hv was employed to induce wear to study the wear characteristics of the samples. The tests were performed using an applied load of 10 N, as shown in Fig. 6. The COF versus the time curve in Figure 4.6a shows that the average COF increased from 0.05 to 0.1, indicating that the wear mechanisms for each alloy were different. The Si<sub>0.4</sub> HEA derivative quenched in water showed the lowest average COF of 0.05, which may be attributed to the dominant BCC phase and the high hardness. All COF curves followed the same trend: first, the coefficient of friction rose rapidly to its maximum value, attributed to the settling of the counter ball on the surface of the HEA sample, and then gradually removed on the worn surface. Afterwards, a gradual decrease was observed to another steady state in sample AlCuFeNiSi<sub>0.4</sub> quenched in oil and aged for 6 hrs attributed to degradation and the greater frictional forces acting on the surface during the running-in period. The wear rate of the heat treated as-cast HEAs in Fig.

6b showed that the Si HEA derivative quenched in water had the lowest wear rates, which is consistent with the hardness and corrosion measurement findings. This may suggest that heat treatments of high entropy alloys are better done with water quenching.

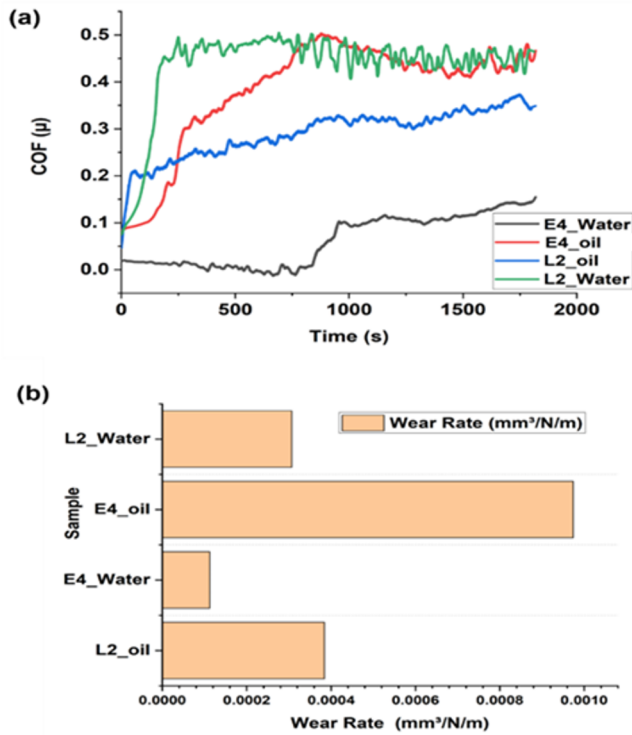


**Fig. 6. a)** Coefficient of friction as a function of sliding distance (b) wear rate of  $\text{AlCuFeNiSi}_{0.4}$  and  $\text{AlCuFeNiTi}_{0.2}$  high entropy alloys at  $750\text{ }^\circ\text{C}$  for 4hrs after quenching in oil and water and aged for 6hr.

The wear mechanism observed from Fig. 7 was abrasive wear. This may be due to the hard small particles embedded on the surface of the alloys. The particles gouged and scratched the metal surface until significant wear and tear.

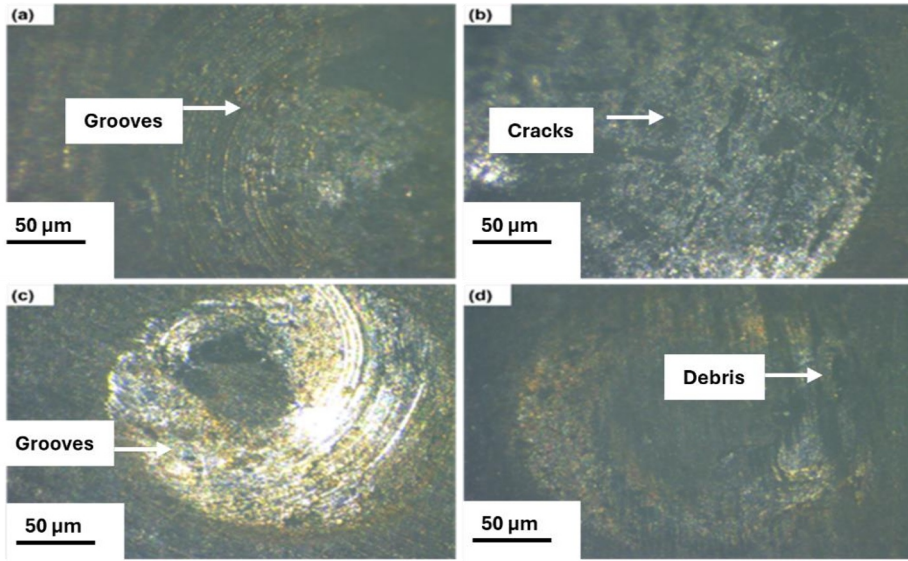


**Fig. 7.** OPM micrographs of the wear subsurface of AlCuFeNiSi<sub>0.4</sub> quenched in oil and aged for 6 hrs (b) OPM micrographs of the wear subsurface of AlCuFeNiTi<sub>0.2</sub> quenched in oil and aged for 6hrs (c) OPM micrographs of the wear subsurface of AlCuFeNiSi<sub>0.4</sub> quenched in water and aged for 6 hrs (d) OPM micrographs of the wear subsurface of AlCuFeNiTi<sub>0.2</sub> quenched in water and aged for 6hrs.

## 4 Conclusion

AlCuFeNiSi<sub>0.4</sub> and AlCuFeNiTi<sub>0.2</sub> quinary HEAs were fabricated using an arc melting technique. Dominant BCC and minor FCC solid solution phases were observed in both alloys. The HEAs quenched in water after ageing showed improved properties compared to those quenched in oil, suggesting that in oil quenched and water quenched, the specimens of arc melted high entropy alloys have better properties in water quenching than oil quenching. Also, the AlCuFeNiSi<sub>0.4</sub> compositions showed more potential for engineering applications with improved properties than the AlCuFeNiTi<sub>0.2</sub> HEA composition.

The authors appreciate the Surface Engineering Research Laboratory, Mintek South Africa, and the Department of Chemical, Metallurgical and Materials Engineering for their technical contribution to this research.

## References

- [1] C.-C. Tung, J.-W. Yeh, T.-t. Shun, S.-K. Chen, Y.-S. Huang, and H.-C. Chen, "On the elemental effect of AlCoCrCuFeNi high-entropy alloy system," *Materials letters*, vol. 61, no. 1, pp. 1-5, 2007.
- [2] S. Huang *et al.*, "Mechanism of magnetic transition in FeCrCoNi-based high entropy alloys," *Materials & design*, vol. 103, pp. 71-74, 2016.

- [3] M. Dada, P. Popoola, and N. Mathe, "Recent advances of high entropy alloys for aerospace applications: a review," *World Journal of Engineering*, vol. 20, no. 1, pp. 43-74, 2023, doi: 10.1108/WJE-01-2021-0040.
- [4] L. Liliensten, J. Couzinié, L. Perrière, J. Bourgon, N. Emery, and I. Guillot, "New structure in refractory high-entropy alloys," *Materials Letters*, vol. 132, pp. 123-125, 2014.
- [5] I. Moravcik, J. Cizek, P. Gavendova, S. Sheikh, S. Guo, and I. Dlouhy, "Effect of heat treatment on microstructure and mechanical properties of spark plasma sintered AlCoCrFeNiTi0.5 high entropy alloy," *Materials Letters*, vol. 174, pp. 53-56, 2016.
- [6] C.-J. Tong, M.-R. Chen, J.-W. Yeh, S.-J. Lin, S.-K. Chen, T.-T. Shun, and S.-Y. Chang, "Mechanical performance of the Al x CoCrCuFeNi high-entropy alloy system with multiprincipal elements," *Metallurgical and Materials Transactions A*, vol. 36, pp. 1263-1271, 2005.
- [7] C.-Y. Hsu, C.-C. Juan, W.-R. Wang, T.-S. Sheu, J.-W. Yeh, and S.-K. Chen, "On the superior hot hardness and softening resistance of AlCoCrFeMo0.5Ni high-entropy alloys," *Materials Science and Engineering: A*, vol. 528, no. 10-11, pp. 3581-3588, 2011.
- [8] C.-y. Hsu, J.-W. Yeh, S.-K. Chen, and T.-T. Shun, "Wear resistance and high-temperature compression strength of Fcc CuCoNiCrAl 0.5 Fe alloy with boron addition," *Metallurgical and Materials Transactions A*, vol. 35, pp. 1465-1469, 2004.
- [9] M.-R. Chen, S.-J. Lin, J.-W. Yeh, M.-H. Chuang, S.-K. Chen, and Y.-S. Huang, "Effect of vanadium addition on the microstructure, hardness, and wear resistance of Al 0.5 CoCrCuFeNi high-entropy alloy," *Metallurgical and Materials Transactions A*, vol. 37, pp. 1363-1369, 2006.
- [10] C.-W. Tsai, M.-H. Tsai, J.-W. Yeh, and C.-C. Yang, "Effect of temperature on mechanical properties of Al0.5CoCrCuFeNi wrought alloy," *Journal of Alloys and Compounds*, vol. 490, no. 1-2, pp. 160-165, 2010.
- [11] É. Fazakas, V. Zadorozhnyy, and D. Louzguine-Luzgin, "Effect of iron content on the structure and mechanical properties of Al25Ti25Ni25Cu25 and (AlTi) 60-xNi20Cu20Fex (x= 15, 20) high-entropy alloys," *Applied Surface Science*, vol. 358, pp. 549-555, 2015.
- [12] W. Guo, J. Li, M. Qi, Y. Xu, and H. R. Ezatpour, "Effects of heat treatment on the microstructure, wear behavior and corrosion resistance of AlCoCrFeNiSi high-entropy alloy," *Intermetallics*, vol. 138, p. 107324, 2021.
- [13] L.R. Kanyanea, A.P.I. Popoolaa, N. Malatji, and M. Dada, "Evaluation of Mechanical and Electrochemical Performance of Arc-melted AlVCrFeNi High Entropy Alloy", In *2024 International Conference on Science, Engineering and Business for Driving Sustainable Development Goals (SEB4SDG) IEEE*, (pp. 1-5), 2024.
- [14] Z. Wang, X. Wang, H. Yue, G. Shi, and S. Wang, "Microstructure, thermodynamics and compressive properties of AlCoCrCuMn-x (x= Fe, Ti) high-entropy alloys," *Materials Science and Engineering, A*, 627, pp.391-398, 2015.
- [15] D. G. Kim *et al.*, "Effects of annealing temperature on microstructures and tensile properties of a single FCC phase CoCuMnNi high-entropy alloy," *Journal of Alloys and Compounds*, vol. 812, p. 152111, 2020.
- [16] S. A. Kube, S. Sohn, D. Uhl, A. Datye, A. Mehta, and J. Schroers, "Phase selection motifs in High Entropy Alloys revealed through combinatorial methods: Large atomic size difference favors BCC over FCC," *Acta Materialia*, vol. 166, pp. 677-686, 2019.

- [17] C.-F. Lee and T.-T. Shun, "Effects of the replacement of Co with Ni on the microstructure, mechanical properties, and age hardening of  $\text{AlCo}_{1-x}\text{CrFeNi}_{1+x}$  high-entropy alloys," *Materials*, vol. 14, no. 10, p. 2665, 2021.
- [18] C.-M. Lin, H.-L. Tsai, and H.-Y. Bor, "Effect of aging treatment on microstructure and properties of high-entropy  $\text{Cu}_{0.5}\text{CoCrFeNi}$  alloy," *Intermetallics*, vol. 18, no. 6, pp. 1244-1250, 2010.
- [19] Y.-F. Kao, T.-D. Lee, S.-K. Chen, and Y.-S. Chang, "Electrochemical passive properties of  $\text{Al}_x\text{CoCrFeNi}$  ( $x= 0, 0.25, 0.50, 1.00$ ) alloys in sulfuric acids," *Corrosion Science*, vol. 52, no. 3, pp. 1026-1034, 2010.